

# Synthesis of superhydrophobic surfaces by polytetrafluoroethylene coating on rectangular grid microstructures

Chao Sun<sup>1</sup>, Inyong Eom<sup>2</sup>, Bonghwan Kim<sup>1</sup> ✉

<sup>1</sup>Department of Electronic and Electrical Engineering, Catholic University of Daegu, Gyeongsan, 38430, Korea

<sup>2</sup>Department of Life Chemistry, Catholic University of Daegu, Gyeongsan, 38430, Korea

✉ E-mail: bhkim@cu.ac.kr

Published in *Micro & Nano Letters*; Received on 17th May 2016; Revised on 28th July 2016; Accepted on 29th July 2016

A simple process to synthesize superhydrophobic surfaces by deep reactive ion etching (DRIE) and polytetrafluoroethylene (PTFE) coating of rectangular grid structures on Si substrate was developed. The Si substrate possesses unique quadrilateral network-type Si microstructures, which when sputtered upon with PTFE, creates a superhydrophobic surface. The fluorinated polymer also exhibited hydrophobic properties where the contact angle of the Si substrate after the PTFE coating was 108.4°. The DRIE etching and PTFE coating together increased the contact angle up to 158.6° for a 40 µm height and 10 × 10 m<sup>2</sup> area, thus synergistically increasing the hydrophobicity of the surface.

**1. Introduction:** Surface wettability is a very important material property concerning real world applications. Recently, due to the potential applications of superhydrophobic surfaces in self-cleaning, anti-fogging, and anti-fouling applications, the study of superhydrophobic surfaces has attracted much attention. [1–5] Superhydrophobic surfaces are those that are extremely difficult to wet, such as leaves of a lotus plant, for which the water droplet contact angle exceeds 150° and the roll-off angle is less than 10° [6]. This is referred to as the Lotus effect [7] and is primarily a physical property related to interfacial tension, rather than a chemical property.

The maximum contact angle that can be achieved by solely applying a hydrophobic coating to a smooth substrate is approximately 120° [8, 9]. Achieving a contact angle greater than 120° using only a chemical treatment on a smooth surface is very difficult. However, in nature, many animals and plants possess superhydrophobic surfaces due to the surface microstructures. The study of biological microstructures has been an active area of research because these microstructures bring about many unique properties [10–18]. For example, plant leaves [11, 12] and insect wings [16] and legs [18] exhibit unusual self-cleaning character, also referred to as the Lotus effect. The lotus leaves can exhibit contact angles of approximately 150°. Therefore, being able to reproduce the lotus effect synthetically would enable creation of superhydrophobic surfaces exhibiting contact angles equal to or greater than 150°. Therefore, to obtain high contact angles similar to that of the lotus leaf, the surfaces must be altered by a microfabrication process. There are two strategies to increase the hydrophobicity of a surface: one is to alter the surface using a physical etching method and the other is to coat the surface using a chemical coating method. The combination of the two methods can synergistically increase the surface hydrophobicity compared with applying the two methods independently. Kwon *et al.* [4] and Lee *et al.* [19] have shown that the network-type microstructures can increase surface hydrophobicity. In order to form superhydrophobic surfaces, they fabricated nano-textured surfaces on top of the microstructures. This significantly enhanced the surface hydrophobicity. The micro-protrusions were able to decrease the contact area between the water droplet and the surface, which also reduces the surface energy and resulting in increased hydrophobicity. However, a drawback to their method is that it requires an extra process to obtain superhydrophobic surfaces. As previously discussed [20–22], we have shown that the combination of micro

and nano-textured structures in combination with a fluorinated polymer coating can maximise hydrophobicity. However, this method still requires a specialised technical process to form the nanostructures on the surface microstructures. In this Letter, we have investigated design parameters (length, width = spacing, and height) using only the microstructure patterning without involving nanostructures to simplify the processing. Specifically, we performed a detailed mechanistic investigation analysing the wettability of solid surfaces as a function of the size of the network-type microstructures. The superhydrophobic surfaces were formed through solid surface etching and coating with a low surface energy chemical coating. The fluorinated polymer also exhibited hydrophobic properties on its own and together with the Si surface having rectangular grid microstructures produced by deep reactive ion etching (DRIE), produced superhydrophobic surfaces [19–22].

**2. Theoretical background and design:** In 1805, Thomas Young [23] defined the contact angle,  $\theta$ , by analysing the forces acting on a fluid droplet resting on a solid surface surrounded by a gas.

$$\cos \theta = (\gamma_{SG} - \gamma_{SL}) / \gamma_{LG} \quad (1)$$

Here,  $\gamma_{SG}$ ,  $\gamma_{SL}$  and  $\gamma_{LG}$  denote the interfacial energy of solid–gas, solid–liquid and liquid–gas, respectively. Young's equation is based on the assumptions that the surface is smooth and that it is homogenous. Thus, for a geometrically rough surface, Young's equation is not valid. To expand upon this, Wenzel [24] determined that when the liquid is in intimate contact with a microstructured surface, as shown in Fig. 1a,  $\theta$  will change to  $\theta_W$

$$\cos \theta_W = (r(\gamma_{SG} - \gamma_{SL})) / \gamma_{LG} = r \cos \theta \quad (2)$$

where  $r$  is the ratio of the actual area to the projected area.

Wenzel's equation shows that micro-structuring of a surface amplifies the natural hydrophobic tendency of the surface. A hydrophobic surface (one that has an original contact angle greater than 90°) becomes more hydrophobic when micro-structured, where its new contact angle becomes greater than the original. However, a hydrophilic surface (one that has an original contact angle less than 90°) will become more hydrophilic when micro-structured resulting in a new contact angle less than the original [25].

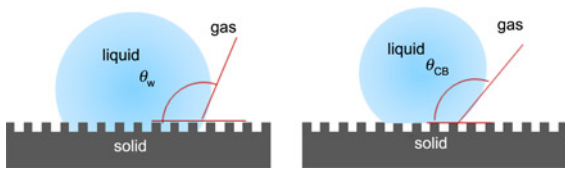


**Fig. 1** Wetting modes of liquid drops on a rough surface  
*a* Wenzel mode  
*b* Cassie–Baxter mode

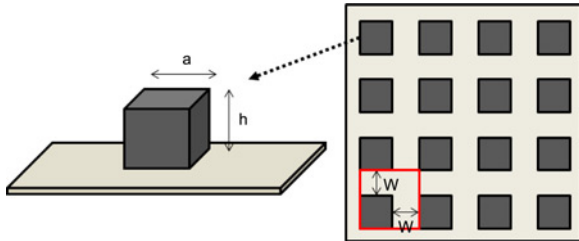


**Fig. 2** Geometry of the designed microstructures

Baxter and Cassie [26] found that if the liquid is suspended on top of the microstructures, as shown in Fig. 1*b*,  $\theta$  will change to  $\theta_{CB}$ .

$$\cos \theta_{CB} = \varphi(\cos \theta + 1) - 1 \quad (3)$$

where  $\varphi$  is the area fraction of the solid that touches the liquid [19].

In this Letter, design parameters for the microstructures are defined in Fig. 2. Three design parameters, the square pillar size ( $a \times a$ ), spacing width ( $w$ ) and height ( $h$ ), are used for the network-type microstructure. The roughness factor ( $r$ ) and solid fraction ( $f$ ) for the wetting modes are functions of these geometric parameters. The roughness factor or the solid fraction of each wetting mode can be expressed as follows:

$$r_w = ((a + w)^2 + 4ah)/(a + w)^2 \quad (4)$$

$$\varphi = a^2/(a + w)^2 \quad (5)$$

In this Letter, the pattern sizes of micro-protrusions in a photomask were designed to be  $10 \times 10 \mu\text{m}$ , where the height of the square pillar ranged from 20 to 60  $\mu\text{m}$  and the width between the square pillars ranged from 25 to 50  $\mu\text{m}$ . The contact angle ( $\theta$ ) of a smooth Si surface coated with polytetrafluoroethylene (PTFE) was measured to be  $108.4^\circ$  and was used for calculations herein. This angle was obtained on a bare Si wafer that was coated with

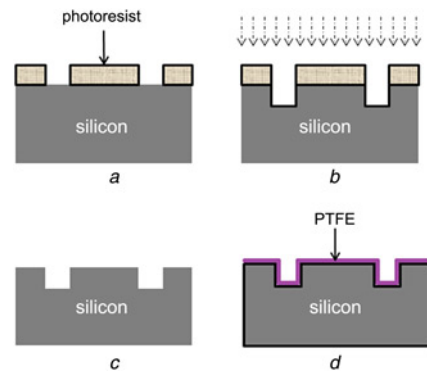


**Fig. 3** Fabrication procedure of microstructures and PTFE coating  
*a* First photolithography  
*b* DRIE  
*c* PR removal  
*d* PTFE coating

a PTFE layer. Table 1 shows the design parameters and calculated contact angles.

**3. Fabrication:** Fig. 3 shows schematic illustrations of the fabrication process of the microstructures. The fabrication procedure starts with photolithography on a 6-inch Si wafer to fabricate the micro-protrusions (Fig. 3*a*). The photoresist (AZ4330, 3  $\mu\text{m}$  thickness) serves as an etch mask in the DRIE procedure (STS Multiplex ICP). The patterned Si surface was then vertically etched to 20, 40, and 60  $\mu\text{m}$  depth, respectively (Fig. 3*b*). After the DRIE, the photoresist was removed in order to make the sample clean (Fig. 3*c*). The fabrication procedure for microstructures was completed upon coating the Si top surfaces with PTFE (Fig. 3*d*).

The PTFE film was coated onto the Si surface by sputtering. Sputtering was carried out under a pure Ar gas atmosphere with a pressure of  $4.2 \times 10^{-2}$  torr and a flow rate of 20 sccm. All films were prepared using an RF power of 50 W, ambient substrate temperature, and deposition time of 10 min [27, 28]. The sample of size  $20 \times 20 \text{ mm}^2$  (actual area is  $10 \times 10 \text{ mm}^2$ ) was parallel to the target surface at a distance of 60 mm.

**4. Results and discussion:** To explore the change of hydrophobicity as a function of surface morphology, the contact angles were measured using a contact angle-meter (DSA100, KRUSS). The water used for measurements of the contact angles was deionised water and the volume was 8  $\mu\text{l}$  (approximate radius of 1.24 mm). The water droplet size can significantly affect the contact angle [29, 30]. The contact angle is known to decrease

**Table 1** Design parameters and calculated contact angles

Theoretical contact angles with respect to the size of microstructures ( $\theta = 108.4^\circ$ )										
Structure size, $\mu\text{m}$		$h = 20 \mu\text{m}$ ( $a, w$ )			$h = 40 \mu\text{m}$ ( $a, w$ )			$h = 60 \mu\text{m}$ ( $a, w$ )		
$a$	$w$	$\theta^w$		$\theta^c$	$\theta^w$		$\theta^c$	$\theta^w$		$\theta^c$
		Calculation	Measurement		Calculation	Measurement		Calculation	Measurement	
10	25	121.5	121.5	160.8	136.7	135.8	160.8	159.1	154.7	160.8
10	30	118.3	118.3	163.2	129.4	128.5	163.2	142.1	140.0	163.2
10	35	116.1	116.1	165.1	124.4	123.9	165.1	133.6	132.2	165.1
10	40	114.6	114.6	166.6	121.2	120.8	166.6	128.2	127.2	166.6
10	45	113.5	113.5	167.8	118.9	118.6	167.8	124.5	123.6	167.8
10	50	112.7	112.7	168.8	117.1	116.9	168.8	121.7	121.1	168.8

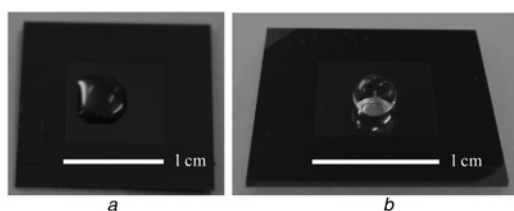
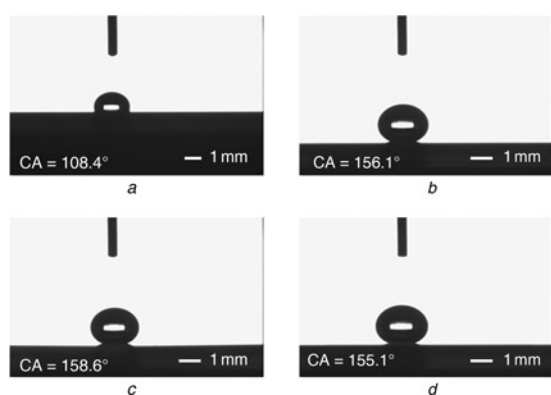


**Fig. 4** Optical image of the 20  $\mu\text{m}$  height and 25  $\mu\text{m}$  width sample with rectangular grid area of 10  $\mu\text{m} \times 10 \mu\text{m}$   
*a* Without PTFE coating  
*b* With PTFE for 10 min

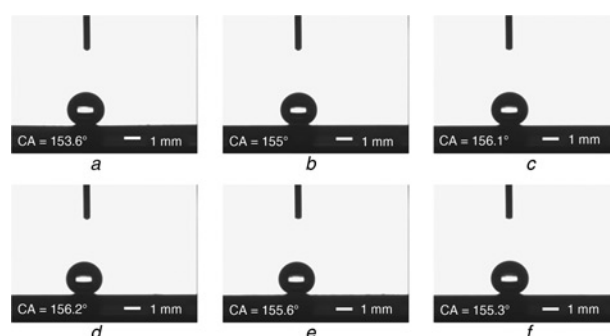
with increasing water droplet sizes [20–22, 29]. Initially, we tested a 3- $\mu\text{l}$  water droplet for measuring contact angle, but the contact angle was immeasurable because the 3- $\mu\text{l}$  water droplet did not stick to the substrate [20–22]. However, Cansoy [30] showed different experimental results between contact angle and water droplet size. Their results showed that an increase or decrease in drop volume had no significant effect on experimentally measured contact angle values of square pillar surfaces with varying pattern sizes [30].

Table 1 summarises the structure sizes and contact angles that were calculated and measured from the microstructures. The reported contact angle was obtained from averaging five measurements.

Fig. 4 shows the water contact angles on microstructures (20  $\mu\text{m}$  height and 25  $\mu\text{m}$  width sample) with and without PTFE coating. The PTFE coated microstructure produces a superhydrophobic surface with a measured contact angle of approximately 155°. Fig. 5 shows the water contact angle of etched Si surfaces with regard to DRIE. The samples were etched with various pillar heights of 20, 40, and 60  $\mu\text{m}$ . The contact angle for the 40  $\mu\text{m}$  height pillar was greater than that of the 20 and 60  $\mu\text{m}$  height pillars. Fig. 6 shows the water contact angle of etched Si surfaces with regard to width between the square pillars. The samples were etched with spacings (i.e. space = width in Fig. 2) between square pillars ranging from 25 to 50  $\mu\text{m}$ . The contact angle for the 35  $\mu\text{m}$  width spacing was significantly higher than those for the other spacings. The contact angle for the PTFE-coated surfaces were over 150°, owing to the microstructure and film thickness. Moreover, the bare Si substrate exhibited hydrophilicity after the formation of an oxide film by contact with the atmosphere. The contact angle of the substrate was approximately 5°, indicating superhydrophilicity [18].



**Fig. 5** Water droplet images on the surface to measure the contact angles with  $a = 10 \mu\text{m}$  and  $w = 25 \mu\text{m}$   
*a* Smooth surface with a contact angle of 108.4°  
*b* 20  $\mu\text{m}$  height of the square pillar surface  
*c* 40  $\mu\text{m}$  height of the square pillar surface  
*d* 60  $\mu\text{m}$  height of the square pillar surface



**Fig. 6** Water droplet images on substrate surfaces to measure the contact angles. Square pillars with surface spacing of  
*a* 25  $\mu\text{m}$   
*b* 30  $\mu\text{m}$   
*c* 35  $\mu\text{m}$   
*d* 40  $\mu\text{m}$   
*e* 45  $\mu\text{m}$   
*f* 50  $\mu\text{m}$  were etched onto the respective surfaces

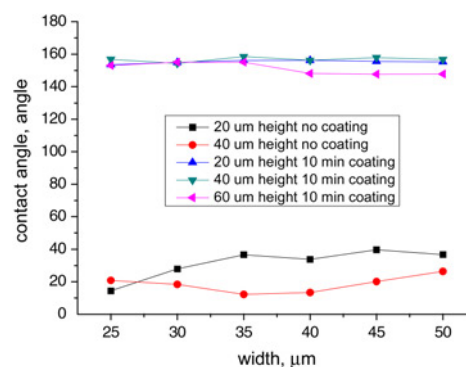


**Fig. 7** Water contact angle as a function of spacing of square pillar surface with  $a = 10 \mu\text{m}$ . (The contact angle of the sample with 60  $\mu\text{m}$  height and without PTFE was less than 5°.)

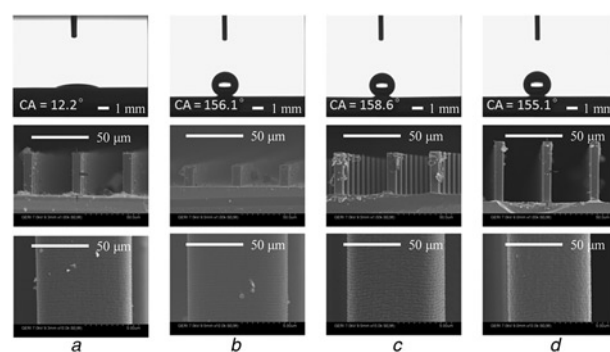


**Fig. 8** Optical images of contact angles and SEM images as a function of pillar height.  
*a* 40  $\mu\text{m}$  height and 35  $\mu\text{m}$  spacing of the square pillar surface without PTFE coating  
*b* 20  $\mu\text{m}$  height and 35  $\mu\text{m}$  spacing of the square pillar surface  
*c* 40  $\mu\text{m}$  height and 35  $\mu\text{m}$  spacing of the square pillar surface  
*d* 60  $\mu\text{m}$  height and 35  $\mu\text{m}$  spacing of the square pillar surface

Fig. 7 summarises the contact angle as a function of spacing of rectangular grid structure. The sample with a 40  $\mu\text{m}$  height and 35  $\mu\text{m}$  spacing produced the highest contact angle. Fig. 8 shows optical images of the contact angles and SEM images as a function of pillar height. After PTFE coating, the surfaces produced contact angles greater than 155° regardless of spacing (width) while the PTFE uncoated surface produced a contact angle of 12.2°.

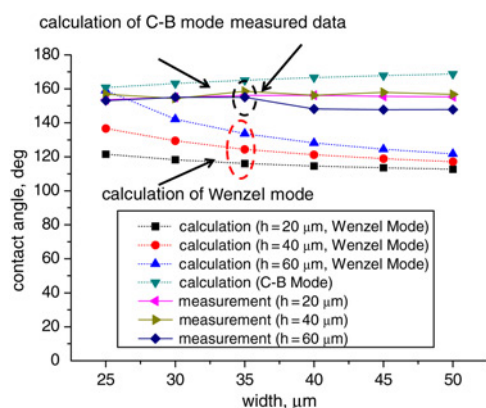


Fig. 9 Water contact angle compared with the Wenzel and C-B mode

Fig. 9 shows the experimentally measured water contact angles in comparison to the Wenzel and the Cassie Baxter (C-B) mode. The measured data is close to the C-B mode but not the Wenzel mode. We conjecture that the difference between the C-B mode and our measured data is due to penetrated water between the square pillars.

**5. Conclusions:** In this Letter, we have developed a surface treatment method for producing superhydrophobic surfaces by the deposition of a PTFE film on Si microstructures. While the maximum contact angle measured from the microstructured surfaces was  $158.6^\circ$ , the minimum measured angle was  $147.7^\circ$ . The difference between the highest and lowest contact angles was  $10.9^\circ$ . The average measured contact angle from the micro-structured surfaces was  $154.4^\circ$ . The sputtering of the PTFE thin film over the micro-textured substrate created a superhydrophobic surface with a water contact angle greater than  $150^\circ$ , which was maintained for 7 weeks. The greatest contact angle was experimentally achieved when the square pillar size ( $a \times a$ ) was  $10 \times 10 \mu\text{m}$ , height ( $h$ ) was  $40 \mu\text{m}$ , and spacing width ( $w$ ) was  $35 \mu\text{m}$ .

**6. Acknowledgments:** This research was supported by Basic Science Research Program through the National Research Foundation of Korea (NRF) funded by the Ministry of Education (grant no. NRF-2013R1A1A4A01012255).

## 7 References

- [1] Bhushan B., Jung Y.C., Koch K.: 'Micro-, nano- and hierarchical structures for superhydrophobicity, self-cleaning and low adhesion', *Philos. Trans. R. Soc.*, 2009, **A 367**, pp. 1631–1672
- [2] Kang C.K., Lee S.M., Jung I.D., *ET AL.*: 'The fabrication of patternable silicon nanotips using deep reactive ion etching', *J. Micromech. Microeng.*, 2008, **18**, p. 075007
- [3] Yan Y., Gao N., Barthlott W.: 'Mimicking natural superhydrophobic surfaces and grasping the wetting process', *Adv. Colloid Interface Sci.*, 2011, **169**, pp. 80–105
- [4] Kwon Y., Patankar N., Choi J., *ET AL.*: 'Design of surface hierarchy for extreme hydrophobicity', *Langmuir*, 2009, **25**, pp. 6129–6136

- [5] He B., Patankar N.A., Lee J.: 'Multiple equilibrium droplet shapes and design criterion for rough hydrophobic surfaces', *Langmuir*, 2003, **19**, pp. 4999–5003
- [6] Wang S., Jiang L.: 'Definition of superhydrophobic states', *Adv. Mater.*, 2007, **19**, (21), pp. 3423–3424
- [7] Lafuma A., Quéré D.: 'Superhydrophobic states', *Nature Mater.*, 2003, **2**, pp. 457–460
- [8] Nakajima A.: 'Design of a transparent hydrophobic coating', *J. Ceram. Soc. Jpn.*, 2004, **112**, pp. 533–540
- [9] Pirat C., Sbragaglia M., Perters A.M., *ET AL.*: 'Multiple time scale dynamics in the breakdown of superhydrophobicity', *Europhys. Lett.*, 2008, **81**, p. 66002
- [10] Barthlott W., Neinhuis C.: 'Purity of the sacred lotus, or escape from contamination in biological surfaces', *Planta*, 1997, **202**, pp. 1–8
- [11] Neinhuis C., Barthlott W.: 'Characterization and distribution of water-repellent, self-cleaning plant surfaces', *Ann. Bot.*, 1997, **79**, (6), pp. 667–677
- [12] Feng L., Li S., Li Y., *ET AL.*: 'Super-hydrophobic surfaces: from natural to artificial', *Adv. Mater.*, 2002, **14**, pp. 1857–1860
- [13] Sun T., Feng L., Gao X., *ET AL.*: 'Bioinspired surfaces with special wettability', *Acc. Chem. Res.*, 2005, **38**, pp. 644–652
- [14] Autumn K., Liang Y.A., Hsieh S.T., *ET AL.*: 'Adhesive force of a single gecko foot-hair', *Nature*, 2000, **405**, pp. 681–685
- [15] Parker A.R., Lawrence C.R.: 'Water capture by a desert beetle', *Nature*, 2001, **414**, pp. 33–34
- [16] Wagner T., Neinhuis C., Barthlott W.: 'Wettability and contaminability of insect wings as a function of their surface sculptures', *Acta Zool.*, 1996, **77**, pp. 213–225
- [17] Gu Z., Uetsuka H., Takahashi K., *ET AL.*: 'Structural color and the lotus effect', *Angew. Chem., Int. Ed. Engl.*, 2004, **42**, pp. 894–897
- [18] Gao X., Jiang L.: 'Biophysics: water-repellent legs of water striders', *Nature*, 2004, **432**, p. 36
- [19] Lee S.M., Jung I.D., Ko J.S.: 'The effect of the surface wettability of nanoprotuberances formed on network-type microstructures', *J. Micromech. Microeng.*, 2008, **18**, p. 125007 (7pp)
- [20] Kim B., Seo S., Bae K., *ET AL.*: 'Stable superhydrophobic Si surface produced by using reactive ion etching process combined with hydrophobic coatings', *Surf. Coat. Technol.*, 2013, **232**, pp. 928–935
- [21] Lee D., Seo S., Kim D., *ET AL.*: 'Nanotextured and polytetrafluoroethylene-coated superhydrophobic surface', *Thin Solid Films*, 2013, **547**, pp. 111–115
- [22] Lee D., Pyo D., Cho C., *ET AL.*: 'Effects on micropylamid and nano-needle structures for superhydrophobicity on Si surface', *Vacuum*, 2016, **131**, pp. 188–193
- [23] Young T.: 'An essay on the cohesion of fluids', *Phil. Trans. R. Soc. Lond.*, 1805, **95**, pp. 65–87
- [24] Wenzel R.N.: 'Resistance of solid surfaces to wetting by water', *Ind. Eng. Chem.*, 1936, **28**, (8), pp. 988–994
- [25] de Gennes P.-G., Brochard-Wyart F., Quere D.: 'Capillarity and wetting phenomena' (Springer Science + Business Media, New York, NY, 2004), ISBN 0-387-00592-7
- [26] Baxter A.B., Cassie S.: 'Wettability of porous surfaces', *Trans. Faraday Soc.*, 1944, **40**, pp. 546–551
- [27] Kim H.M., Sohn S., Ahn J.S.: 'Transparent and super-hydrophobic properties of PTFE films coated on glass substrate using RF-magnetron sputtering and Cat-CVD methods', *Surf. Coat. Technol.*, 2013, **228**, pp. S389–S392
- [28] Kong D., Oh J., Pyo D., *ET AL.*: 'Fabrication of Nano-sized silicon surface structure with lowest reflectance by reactive ion etching method', *Jpn. J. Appl. Phys.*, 2013, **52**, p. 06GL06 (7 pages)
- [29] Gaydos J., Neumann A.W.: 'The dependence of contact angle on drop size and line tension', *J. Colloid Interface Sci.*, 1987, **120**, (1), pp. 76–86
- [30] Cansoy C.E.: 'The effect of drop size on contact angle measurements of superhydrophobic surfaces', *RSC Adv.*, 2014, **4**, pp. 1197–1203